

## Design of a boiling water reactor equilibrium core using thorium-uranium fuel

Juan-Luis François<sup>1</sup>, Alejandro Núñez-Carrera<sup>1,2</sup>,  
Gilberto Espinosa-Paredes<sup>3</sup>, Cecilia Martín-del-Campo<sup>1</sup>

<sup>1</sup>Universidad Nacional Autónoma de México – Facultad de Ingeniería. Paseo Cuauhnáhuac 8532, 62550 Jiutepec, Mor. México. francois@premia.imta.mx, cmcm@fi-unam.mx

<sup>2</sup>Comisión Nacional de Seguridad Nuclear y Salvaguardias. Dr. Barragán 779 Col. Narvarte, 03020 México, D. F. México. anunezc@cnsns.gob.mx

<sup>3</sup>Universidad Autónoma Metropolitana, División de Ciencias Básicas e Ingeniería, Av. San Rafael Atlixco 186, Col. Vicentina, 09340 México, D.F. México. gepe@xanum.uam.mx

### Abstract

In this paper the design of a Boiling Water Reactor (BWR) equilibrium core using thorium is presented; a heterogeneous blanket-seed core arrangement concept was adopted. The design was developed in three steps: in the first step two different assemblies were designed based on the integrated blanket-seed concept, they are the blanket-dummy assembly and the blanket-seed assembly. The integrated blanket-seed concept comes from the fact that the blanket and the seed rods are located in the same assembly, and are burned-out in a once-through cycle.

In the second step, a core design was developed to achieve an equilibrium cycle of 365 effective full power days in a standard BWR with a reload of 104 fuel assemblies designed with an average <sup>235</sup>U enrichment of 7.5 w/o in the seed sub-lattice. The main operating parameters, like power, linear heat generation rate and void distributions were obtained as well as the shutdown margin. It was observed that the analyzed parameters behave like those obtained in a standard BWR. The shutdown margin design criterion was fulfilled by addition of a burnable poison region in the assembly.

In the third step an in-house code was developed to evaluate the thorium equilibrium core under transient conditions. A stability analysis was also performed.

Regarding the stability analysis, five operational states were analyzed; four of them define the traditional instability region corner of the power-flow map and the fifth one is the operational state for the full power condition. The frequency and the boiling length were calculated for each operational state. The frequency of the analyzed operational states was similar to that reported for BWRs; these are close to the unstable region that occurs due to the density wave oscillation phenomena in some nuclear power plants. Four transient analyses were also performed: manual SCRAM, recirculation pumps trip, main steam isolation valves closure and loss of feed water. The results of these transients are similar to those obtained with the traditional UO<sub>2</sub> nuclear fuel.

### 1. INTRODUCTION

The use of thorium as a nuclear material in light and heavy water reactors has taken a new interest because of the potential advantages that can be obtained from this fuel cycle [1,2,3]. For instance, it can be first mentioned that the thorium cycle is an easy way to improve the fuel conversion in a once-through cycle in the thermal reactors. Second, the thorium cycle tend to reduce the proliferation of spent fuel, it is much more favorable in plutonium contents, decay heat amount and radioactivity level from spent fuels. Third, the thorium cycle improves the long-lived minor actinides production compared with the uranium and plutonium cycle; the radiotoxicity level of spent fuel is less in thorium cycle than the others, in case of once-through cycle application for LWR.

Nowadays three main research areas related with the thorium fuel cycle are in progress in different universities or laboratories around the world. The accelerator driven systems (ADS) in which the thorium breeding capability is achieved by the neutrons obtained by the spallation reaction from the particles obtained from the accelerator. The breeder reactors in which the burned fuel is reprocessed in order to recover the U-233 produced from the Th-232 conversion. The third research area deals with actual nuclear reactors, mainly PWR, BWR and CANDU, in which innovative thorium-uranium and thorium-plutonium fuel designs are in development trying to improve the fuel cycle performance, safety and economy.

We are interested in the third area and as part of a project to investigate energy systems based on the thorium fuel cycle; an innovative thorium-uranium fuel was designed to be used in a BWR-type equilibrium core (actual BWR, ABWR or SBWR). The design was developed in three steps: in the first step two different assemblies were designed based on the integrated blanket-seed concept, they are the blanket-dummy assembly and the blanket-seed assembly. In the second step, a core design was developed to achieve an equilibrium cycle of 365 effective full power days in a standard BWR. In the third step the thorium equilibrium core under transient conditions was analyzed. A stability analysis was also performed.

## 2. FUEL LATTICE DESIGN

The proposed lattice design use the blanket-seed concept [4, 5] in a triangular lattice pitch, which includes the blanket and the seed rods (figure 1) in a heterogeneous loading fashion. The blanket rods has only thorium in the form of  $\text{ThO}_2$  and the seed rods contain metal fuel in the form of uranium-zirconium alloy (U/Zr), as it is proposed in reference 4 and 5. The so defined triangular blanket-seed lattice is composed by the blanket sub-lattice and the seed sub-lattice. The fresh blanket sub-lattice will be first loaded in the core (one cycle) to produce its own fissile fuel (mainly U-233). At this step a dummy zircaloy rod instead of the seed rod occupies the center of the triangular lattice. At the next cycle the blanket sub-lattice will be assembled with the fresh seed sub-lattice to form the blanket-seed lattice (the zircaloy sub-lattice is retired at this time). The advantage to have the blanket-seed rods in the same fuel assembly is to reduce the power mismatch between blanket assemblies and seed assemblies presented in other designs. A mismatch between blanket and seed rods is expected to occur in the lattice, nevertheless we can take advantage of the higher thermal conductivity of the U/Zr seed rods ( $0.18 \text{ W/cm}^\circ\text{C}$  [6]) compare with the  $\text{ThO}_2$  blanket rods ( $0.04 \text{ W/cm}^\circ\text{K}$  [7]) to produce more power in the seed rods.

The fuel design process was carried out in several steps. In the first step, the pitch was selected in the triangular blanket-seed lattice. In the second step, the blanket composition was determined in order to improve the U-233 build-up from Th-232 conversion. In the third step, the uranium to zirconium ratio and the final seed and dummy rods diameters were determined in order to have the “better” neutronic performance,  $K_{\text{inf}}$  vs burn-up and void reactivity coefficient for a typical BWR.

### 2.1 PITCH SELECTION IN THE BLANKET-SEED LATTICE

In this step, several calculations were done with different pitch sizes. The pitch in the blanket-seed lattice is defined as the distance between blanket rods (center to center). The dimensions of a standard BWR assembly must be taken into account in the final pitch selection, since a regular array of blanket-seed cells must be fixed in the assembly. Figure 2 shows the k-infinite values obtained for different pitch sizes and for different void percentages.

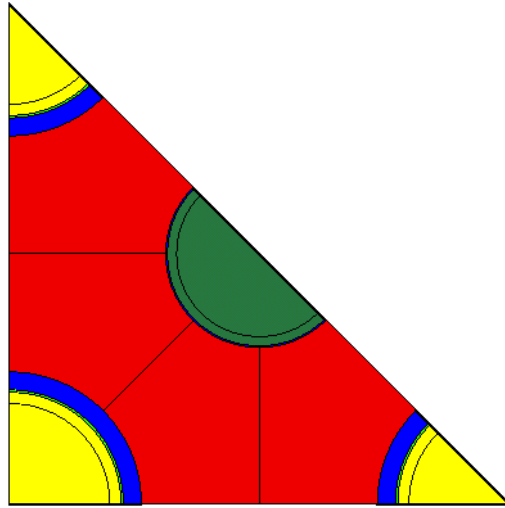


Figure 1. Blanket (yellow edge rods) – seed (central green rod) lattice. Helios representation, reflective boundary condition (Orion view).

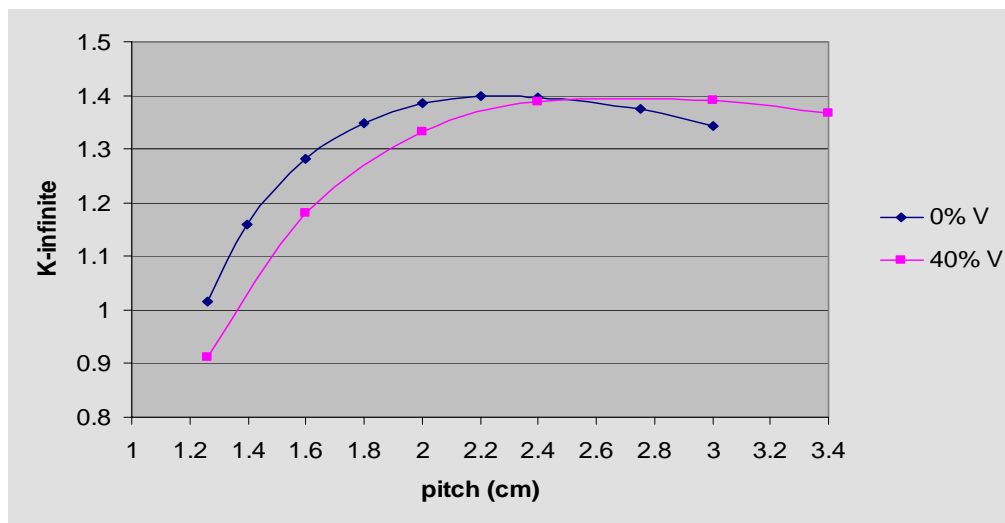


Figure 2. Pitch sensitivity calculations.

Taking into account the results of figure 2 and the criteria of the BWR assembly dimensions, a pitch of 1.91 cm was selected, which allows to accommodate a 7x7 array of blanket rods and a 6x6 embedded array of seed rods (see figure 3). On the other hand the selected pitch is in the under-moderated region of the k-infinite vs pitch curve ensuring a safe behavior of the moderator reactivity coefficient.

## 2.2 BLANKET SELECTION

One of the goals of the blanket-seed design presented in this work is to improve the U-233 production of the blanket sub-lattice, which will be loaded in the core (in the periphery when they are fresh) during one operating cycle. Therefore we tried to find the better blanket composition that will improve the conversion. Figure 4 shows the main fissile isotopes evolution in the blanket sub-lattice. Three different cases are presented: U233\_Unat represents a blanket with 90% ThO<sub>2</sub> and 10% natural uranium. U233\_10%U25 is a blanket with 90% ThO<sub>2</sub> and 10% uranium enriched at 10% in U-235 and U233\_ThO2

is the blanket with 100% ThO<sub>2</sub>. It can be seen how the last case has the higher rate conversion of Th-232 to U-233 and reduce the plutonium production. Therefore this last blanket composition was chosen.

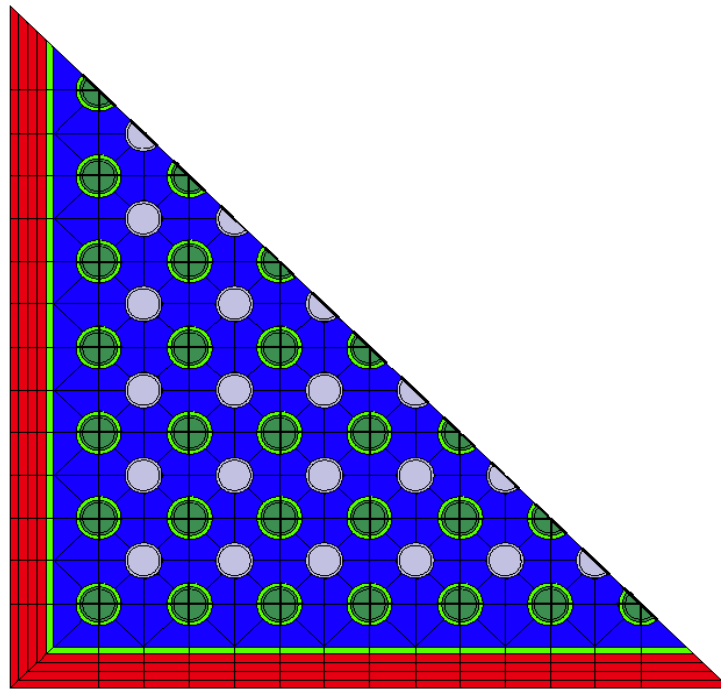


Figure 3. Blanket-seed lattice (diagonal symmetry).

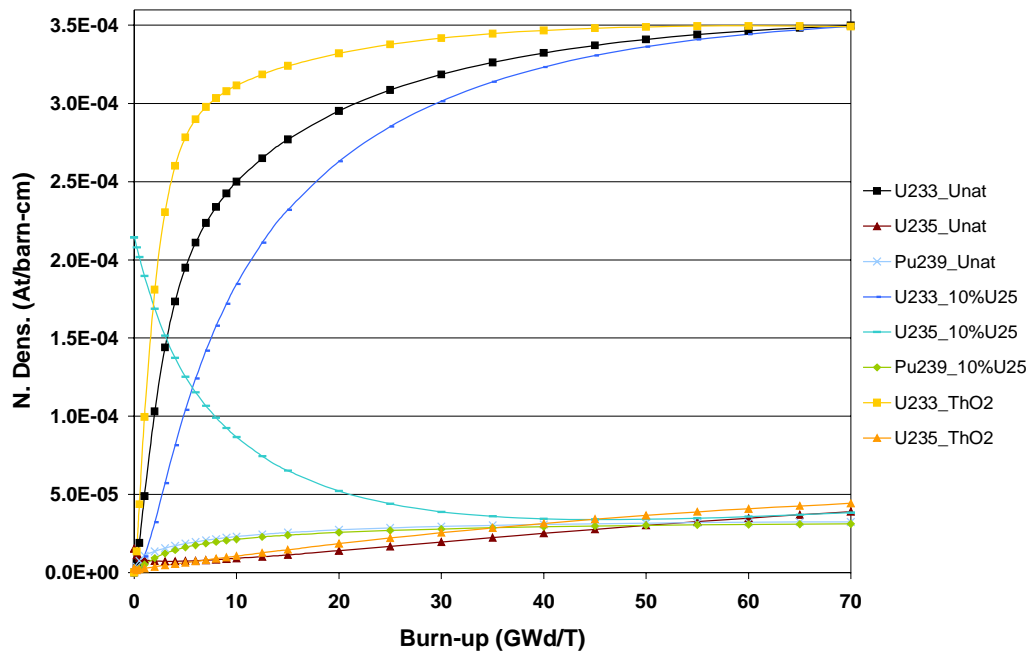


Figure 4. Main fissile isotopes evolution in the blanket sub-lattice

## 2.3 SEED COMPOSITION AND DIAMETER DETERMINATION

At this step, the blanket-seed lattice was defined from the neutronic point of view. The selected U/Zr alloy is composed by 80% uranium and 20% zirconium. This proportion provides a high alloy density (16.5 g/cc), which permits a reduction in the seed U-235 enrichment and a small rod diameter (0.8 cm). This seed rod diameter gives a good reactivity performance, as can be seen in figure 5. Rods with higher dimension could provide better reactivity performance; nevertheless they would have a higher power production that could produce thermal limits problems and they would significantly reduce the coolant flow area jeopardizing the fuel cooling capability. The final dummy rod diameter is chosen to be the same as the seed rod, in order to avoid mechanical troubles when the dummy rods will be changed by the seed rods.

The reactivity performance of the blanket-seed lattice is shown in figure 6, where the k-infinite vs burn-up is shown at hot full power conditions and 40% voids, for the following equivalent BWR lattice types:

- Lat3 = triangular blanket-seed lattice where the blanket is first burned one cycle and the seed is loaded afterwards. The seed U-235 enrichment is 5.5%. The blanket sub-lattice was burned up to 9,000 MWd/T before being assembled with the fresh seed sub-lattice.
- Lat4 = triangular blanket-seed lattice where the blanket and the seed are both loaded fresh together since beginning of life. The seed U-235 enrichment is 5.5%.
- UO<sub>2</sub>\_3.37 = regular rectangular lattice of uranium oxide fuel. The U-235 enrichment is 3.37 %.
- MOX\_3.93 = regular rectangular lattice of a mixed oxide fuel of plutonium and uranium. The Pu fissile enrichment is 3.93 %.

As can be seen in figure 6, the proposed design (Lat3) has a good reactivity performance with a relative low U-235 enrichment (5.5%), even more if we take into account that the seed represents only 42% of the lattice volume. The Lat4 case does not reaches the required reactivity.

Regarding the reactivity void coefficient, the proposed blanket-seed lattice has always a negative value: -240 pcm at BOL and -54 pcm at 60,000 MWd/T.

Concerning the isotopic inventory of the blanket-seed assembly, it must be noticed that the actinides concentration is reduced considerably as the fuel burns out, compared with uranium and MOX fuel. Table I shows the isotopic composition in weight percent of three equivalent fuel assemblies. It can be observed that the total amount of transuranic isotopes at the end of life (EOL) is considerably lower in the Th-U assembly than the others; it is more or less the half of the uranium assembly.

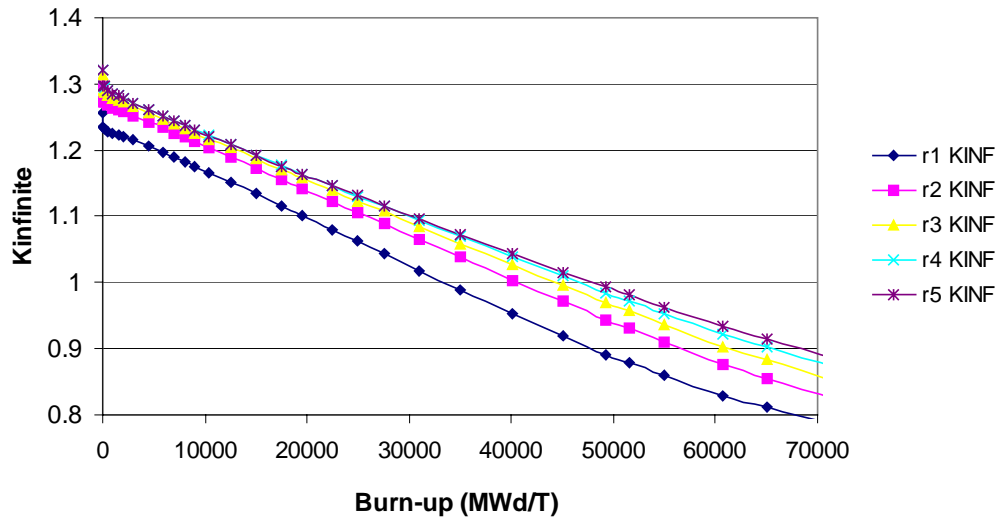


Figure 5. K-infinite vs burn-up for different seed rod dimensions.  
 (r1=0.33cm, r2=0.4cm, r3=0.45cm, r4=0.5cm, r5=0.55cm)

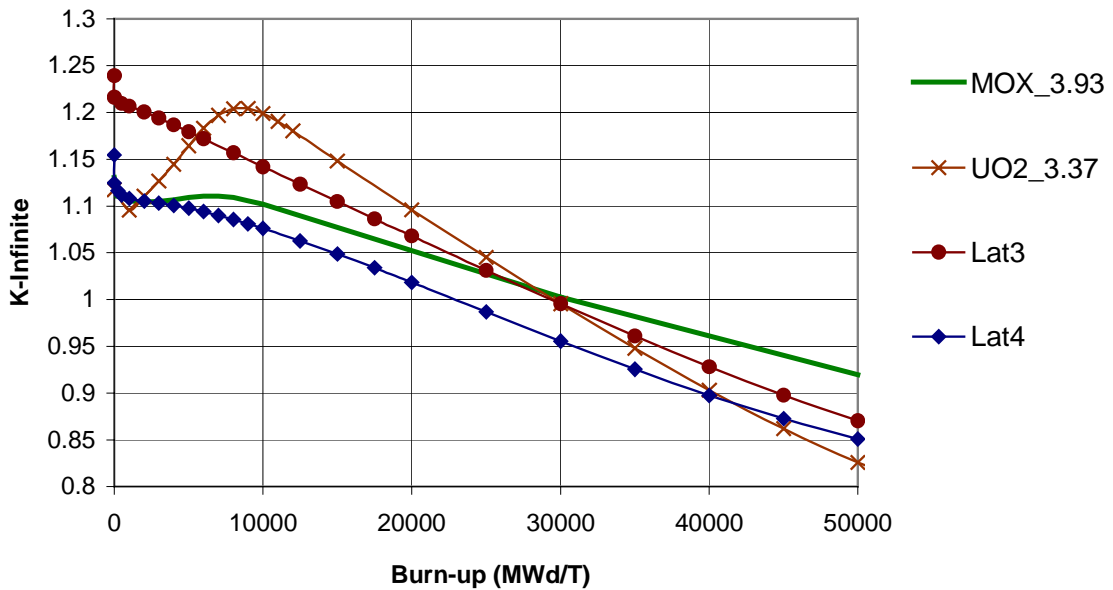


Figure 6. Blanket-seed lattice reactivity performance.

**Table I.** Isotopic composition (w/o) for different fuel assembly types.

| Ass. type                 | UO <sub>2</sub> |          |         | ThO <sub>2</sub> +UZr |          |         | UO <sub>2</sub> +PuO <sub>2</sub> |          |         |
|---------------------------|-----------------|----------|---------|-----------------------|----------|---------|-----------------------------------|----------|---------|
|                           | BOL             | 30 GWd/T | EOL*    | BOL                   | 30 GWd/T | EOL*    | BOL                               | 30 GWd/T | EOL*    |
| Pa233                     |                 |          |         |                       | 0.0332   | 0.0398  |                                   |          |         |
| U233                      |                 |          |         |                       | 0.6889   | 0.6950  |                                   |          |         |
| U235                      | 3.3673          | 0.9766   | 0.1892  | 2.9549                | 1.0257   | 0.0479  | 0.4294                            | 0.2354   | 0.1223  |
| Pu239                     |                 | 0.4192   | 0.3837  |                       | 0.2120   | 0.1998  | 3.0452                            | 1.8360   | 1.2307  |
| Pu241                     |                 | 0.0900   | 0.1238  |                       | 0.0408   | 0.0615  | 0.8832                            | 0.8166   | 0.6690  |
| Th232                     |                 |          |         | 46.3678               | 44.0769  | 42.8021 |                                   |          |         |
| Pa231                     |                 |          |         |                       | 0.0027   | 0.0032  |                                   |          |         |
| U232                      |                 |          |         |                       | 0.0289   | 0.0039  |                                   |          |         |
| U234                      |                 |          |         |                       | 0.0021   | 0.1893  |                                   |          |         |
| U236                      |                 | 0.3952   | 0.4667  |                       | 0.1313   | 0.0177  |                                   | 0.0392   | 0.0560  |
| U238                      | 96.6327         | 94.7530  | 92.6389 | 50.6773               | 49.7862  | 48.8677 | 92.9793                           | 91.2278  | 89.5673 |
| Np237                     |                 | 0.0311   | 0.0596  |                       | 0.0196   | 0.0388  |                                   | 0.0107   | 0.0187  |
| Np238                     |                 |          |         |                       | 0.0000   | 0.0001  |                                   |          |         |
| Np239                     |                 |          |         |                       | 0.0019   | 0.0023  |                                   |          |         |
| Pu238                     |                 | 0.0089   | 0.0329  |                       | 0.0003   | 0.0008  | 0.1450                            | 0.1271   | 0.1408  |
| Pu240                     |                 | 0.1902   | 0.2841  |                       | 0.0932   | 0.1446  | 1.9378                            | 1.7251   | 1.4073  |
| Pu242                     |                 | 0.0324   | 0.1229  |                       | 0.0133   | 0.0518  | 0.5800                            | 0.6891   | 0.7959  |
| Am241                     |                 | 0.0032   | 0.0049  |                       | 0.0019   | 0.0036  |                                   | 0.0842   | 0.0881  |
| Am243                     |                 | 0.0050   | 0.0320  |                       | 0.0018   | 0.0117  |                                   | 0.1100   | 0.1745  |
| Cm242                     |                 | 0.0009   | 0.0025  |                       | 0.0004   | 0.0012  |                                   | 0.0109   | 0.0161  |
| Cm244                     |                 | 0.0011   | 0.0171  |                       | 0.0004   | 0.0051  |                                   | 0.0402   | 0.1122  |
| <b>Total Transuramics</b> |                 | 0.2727   | 0.5560  |                       | 0.1327   | 0.2598  | 2.6629                            | 2.7866   | 2.7349  |

\*EOL=55 GWd/T

With these blanket-seed and blanket-dummy assemblies, a core design was developed to achieve an equilibrium cycle in a standard BWR.

### 3. EQUILIBRIUM CORE DESIGN

The core of Laguna Verde Nuclear Power Plant (Mexican nuclear power plant) was chosen as a base case for the design of a typical BWR core. This is a small core with 444 fuel assemblies, rated at 2027 MWth, therefore the challenge is to locate the blanket-dummy assemblies and the blanket-seed assemblies in such way to achieve the <sup>233</sup>U breeding while keeping a reasonable power distribution to obtain a desired cycle length. The calculations were performed with the CM-PRESTO [8], which is a three dimensional neutronic-thermalhydraulic steady state simulator. The nuclear data banks were generated with the HELIOS [9] system and they were processed by TABGEN [10] to produce tables of nuclear cross sections depending on burn-up, void and exposure weighted void (void history) which are used by CM-PRESTO. The Haling strategy was used in order to obtain an equilibrium cycle length of 365 effective full power days (EFPD) with an assumed end of cycle target eigenvalue. In a multi-cycle procedure, a sufficient

number of cycles were run until no changes were observed in cycle length, power distribution, burn-up and void distribution in the core.

The general loading strategy is as follows: the fresh blanket-dummy assemblies are first loaded in the core (one cycle) to produce its own fissile fuel (mainly  $^{233}\text{U}$ ). At the next cycle the blanket sub-lattice will be assembled with the fresh seed sub-lattice to form the blanket-seed lattice (the zircaloy sub-lattice is retired at this time) and relocated in the core. The advantage to have the blanket-seed rods in the same fuel assembly is to reduce the power mismatch between blanket assemblies and seed assemblies presented in other designs [4, 5].

An equilibrium reload of 104 fuel assemblies was designed with an average  $^{235}\text{U}$  enrichment of 7.5 w/o in the seed sub-lattice to obtain a cycle length of 365 EFPD; the fresh blanket sub-lattice has only  $\text{ThO}_2$  rods. Figure 7 shows the location of the different fuel assemblies and the average relative power distribution per assembly; Figure 8 shows the axial power distribution. The blanket-dummy assemblies are mainly located in the core periphery to serve as reflector at the same time they are used to convert the  $^{232}\text{Th}$  into  $^{233}\text{U}$ . The fresh blanket-seed assemblies (the most reactive) have to be located close to the periphery to improve the breeding of the blanket-dummy assemblies and to flatten the radial power distribution; using the "ring of fire" concept. The rest of the assemblies are located in the core in order to obtain a smooth power distribution and to get the desired cycle length.

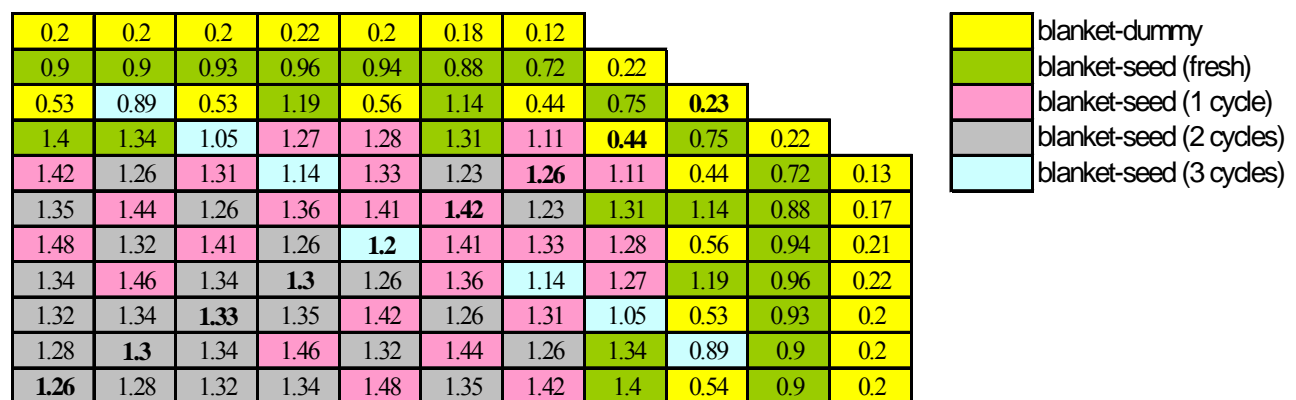


Figure 7. Core design and relative power distribution.

The relative power distributions showed in the previous figures present quite standard values for a Haling type calculation in a BWR, and not high power peaking values were observed between different assembly types.

Next Figures (9, 10, 11 and 12) show the linear heat generation rate and the void fraction distributions. The values presented in these figures are also fairly standard values for a Haling type calculation in a BWR.



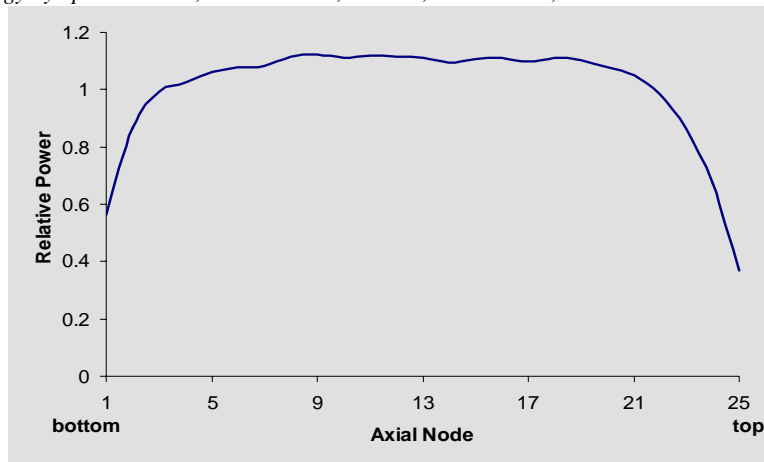


Figure 8. Relative axial power distribution.

|            |     |     |     |            |     |     |     |     |     |    |
|------------|-----|-----|-----|------------|-----|-----|-----|-----|-----|----|
| 51         | 52  | 53  | 57  | 53         | 47  | 30  |     |     |     |    |
| 151        | 151 | 156 | 161 | 158        | 148 | 122 | 57  |     |     |    |
| 141        | 118 | 139 | 197 | 148        | 190 | 116 | 127 | 61  |     |    |
| 228        | 219 | 140 | 196 | 196        | 216 | 167 | 117 | 127 | 57  |    |
| 213        | 170 | 192 | 152 | 196        | 167 | 195 | 167 | 116 | 122 | 33 |
| 183        | 217 | 170 | 198 | 212        | 216 | 167 | 216 | 190 | 149 | 44 |
| <b>221</b> | 178 | 208 | 171 | 161        | 212 | 196 | 196 | 148 | 159 | 54 |
| 181        | 219 | 183 | 176 | 171        | 198 | 152 | 196 | 197 | 161 | 57 |
| 180        | 185 | 181 | 186 | 208        | 170 | 192 | 140 | 139 | 156 | 53 |
| 173        | 177 | 185 | 219 | 178        | 217 | 170 | 220 | 118 | 151 | 52 |
| 171        | 173 | 180 | 181 | <b>221</b> | 183 | 213 | 228 | 141 | 152 | 51 |

Figure 9. Radial linear heat generation rate distribution (w/cm).

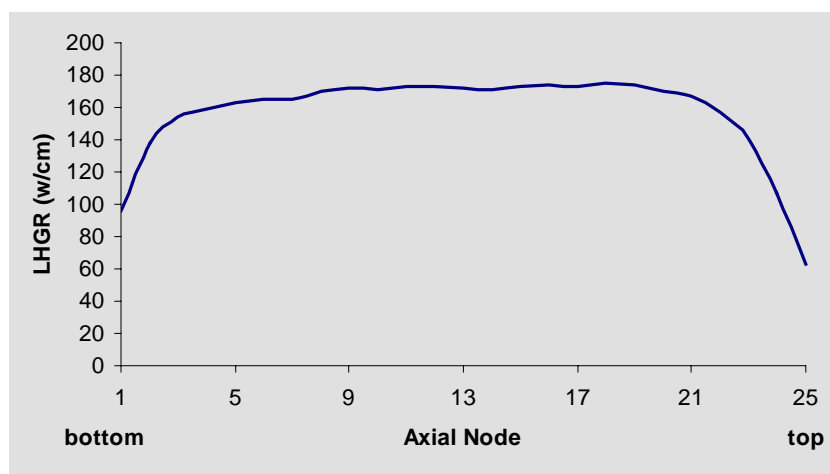


Figure 10. Axial linear heat generation rate distribution.

|      |      |      |      |      |      |      |      |      |      |      |
|------|------|------|------|------|------|------|------|------|------|------|
| 0.17 | 0.25 | 0.29 | 0.30 | 0.28 | 0.23 | 0.14 |      |      |      |      |
| 0.20 | 0.31 | 0.33 | 0.33 | 0.32 | 0.30 | 0.24 | 0.34 |      |      |      |
| 0.35 | 0.37 | 0.41 | 0.38 | 0.38 | 0.37 | 0.33 | 0.28 | 0.37 |      |      |
| 0.41 | 0.45 | 0.40 | 0.46 | 0.43 | 0.45 | 0.38 | 0.32 | 0.28 | 0.34 |      |
| 0.47 | 0.45 | 0.48 | 0.46 | 0.49 | 0.48 | 0.38 | 0.38 | 0.33 | 0.24 | 0.16 |
| 0.41 | 0.49 | 0.47 | 0.50 | 0.47 | 0.50 | 0.48 | 0.45 | 0.37 | 0.30 | 0.22 |
| 0.48 | 0.46 | 0.50 | 0.49 | 0.51 | 0.47 | 0.49 | 0.43 | 0.38 | 0.32 | 0.29 |
| 0.42 | 0.49 | 0.44 | 0.50 | 0.45 | 0.50 | 0.46 | 0.46 | 0.39 | 0.34 | 0.31 |
| 0.48 | 0.46 | 0.49 | 0.44 | 0.50 | 0.47 | 0.49 | 0.41 | 0.42 | 0.34 | 0.30 |
| 0.41 | 0.48 | 0.46 | 0.49 | 0.47 | 0.50 | 0.46 | 0.46 | 0.38 | 0.32 | 0.27 |
| 0.38 | 0.41 | 0.48 | 0.43 | 0.50 | 0.47 | 0.49 | 0.42 | 0.36 | 0.22 | 0.21 |

Figure 11. Radial void fraction distribution.

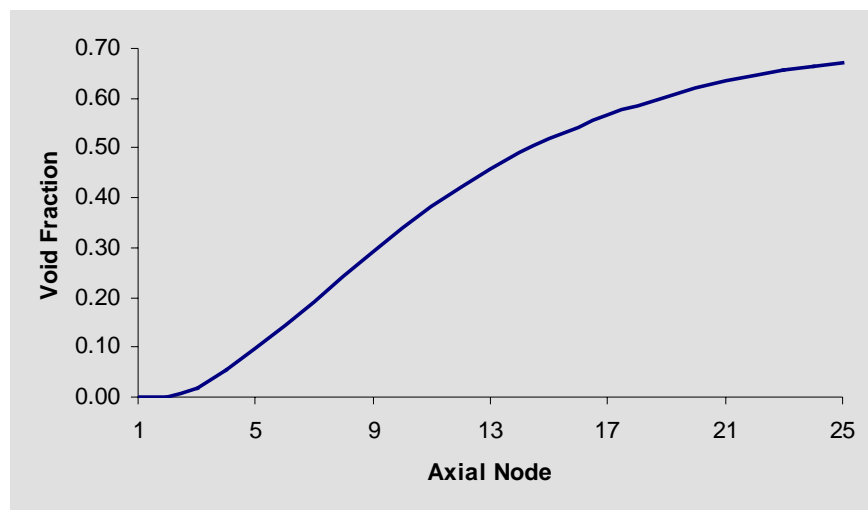


Figure 12. Axial void fraction distribution.

Regarding shutdown margin, the value obtained with the equilibrium core design was 0.89%  $\Delta k/k$  at beginning of cycle, which is higher than the 0.37%  $\Delta k/k$  value of the technical specification but it is lower than the 1%  $\Delta k/k$  used for design purposes.

In order to improve the shutdown margin some options were analyzed. In the first one, ten gadolinia ( $Gd_2O_3$ ) burnable poison rods at 1% were included in one of the upper nodes of the fuel assembly. In the second option, natural uranium fuel rods were included in the top and the bottom nodes of the fuel assembly (in our core analysis, the assembly was divided in 25 axial nodes). These options were analyzed with CM-PRESTO at cold zero power condition with all control rods inserted (ARI) and the strongest rod out (SRO). The analyzed cases were the following:

- Case 1:** Original case without gadolinia rods, without natural uranium.
- Case 2:** 10 gadolinia rods at 1% were added to the fuel assembly in one of the upper nodes, without natural uranium.
- Case 3:** 1 node with natural uranium in the bottom and 2 nodes with natural uranium in the top of the fuel assembly were added. No gadolinia rods.
- Case 4:** 1 node with natural uranium in the bottom and 1 node with natural uranium in the top of the fuel assembly were added. No gadolinia rods.
- Case 5:** 1 node with natural uranium in the top of the fuel assembly was added. No gadolinia rods.

Table II shows the cold zero power (xenon free) neutron multiplication factor for ARI and SRO condition for the different cases. Shutdown margin and cycle length, obtained with the modified fuel assemblies in the core, are also shown in Table I. Case 1 corresponds to the original design, the rest of the cases satisfy the shutdown margin criteria,  $\Delta k/k > 1$ . Finally case 2 was selected because it satisfies the shutdown margin and has the longest cycle, equivalent to the original case.

Table II. Infinite neutron multiplication factor for SDM calculations.

| Case | ARI    | SRO    | SDM<br>% $\Delta k/k$ | Cycle length<br>(days) |
|------|--------|--------|-----------------------|------------------------|
| 1    | 0.9858 | 0.9912 | 0.89                  | 370                    |
| 2    | 0.9778 | 0.9836 | 1.67                  | 370                    |
| 3    | 0.9173 | 0.9635 | 3.79                  | 341                    |
| 4    | 0.9190 | 0.9605 | 4.11                  | 353                    |
| 5    | 0.9361 | 0.9652 | 3.61                  | 365                    |

#### 4. TRANSIENT AND STABILITY ANALYSIS

An in-house code was developed to evaluate the thorium equilibrium core under steady state and transient conditions; a stability analysis was also performed. The reactor vessel was divided into five zones. Two of these zones, the vessel dome and the downcomer, have a variable volume. The three fixed-volume zones are the lower plenum, which includes the jet pump volume, the upper plenum and the steam separator, and the reactor core. The reactor core was divided into 12 one-dimensional nodes. The reactor model is completed with the two recirculation loops, the neutron kinetics and the fuel rod transient temperatures models. The fuel element is represented by a one-dimensional mesh-centered grid consisting of 8 radial nodes for each element of the grid. The differential equations are transformed into discrete equations using the control volume formulation technique in implicit form. The code also includes a control model (level and pressure) and a simplified model of feed water and main steam.

The code has two modules: a) the time domain module for transient analysis and b) the frequency domain module for stability analysis. Thermalhydraulic effects are modeled by a set of five equations [11]. The neutronic phenomena are calculated with a point kinetics model. Typical BWR reactivity effects are considered: void fraction, fuel temperature, moderator temperature and control rod density (0 means no control rods inserted and 1 means all rods totally inserted). Collapsed parameters were included in the code to represent the core with an average fuel channel. For the stability analysis, in the frequency domain, the model of Lahey and Podowski [12] was used, where the system transfer function is

determined by applying Laplace-transforming to the calculated pressure drop perturbations in each of the considered regions; the assumption of a constant total pressure drop was applied. The transfer function was used to study the system response in the frequency domain when an inlet flow perturbation is applied. The expected results using point kinetics are conservative compared with those obtained with three dimensional calculations. This is an important result of the Main Steam Line Break Benchmark analysis organized by Pennsylvania State University and the Nuclear Energy Agency of the OECD [13].

Four transient analyses were also performed: manual SCRAM, recirculation pumps trip, main steam isolation valves closure and loss of feed water. The results of these transients simulation are similar to those obtained with the traditional  $UO_2$  nuclear fuel. For instance, for the main steam isolation valves closure transient, the safety relief valves (SRV's) opened in order to control the overpressure in the vessel, as shown in Figures 14 and 15.

Regarding the instability analysis, five operational states were analyzed; four of them define the traditional instability region corner of the power-flow map and the fifth one is the operational state for the full power condition. The frequency and the boiling length were calculated for each operational state (Table III). The frequency of the operational states 1, 2, 3 and 4 are similar to that reported by other authors [14, 15]; these are close to the unstable region that occurs due to the density wave oscillation phenomena in some nuclear power plants. The results for a standard uranium core ( $UO_2$ ) are also shown in Table III.

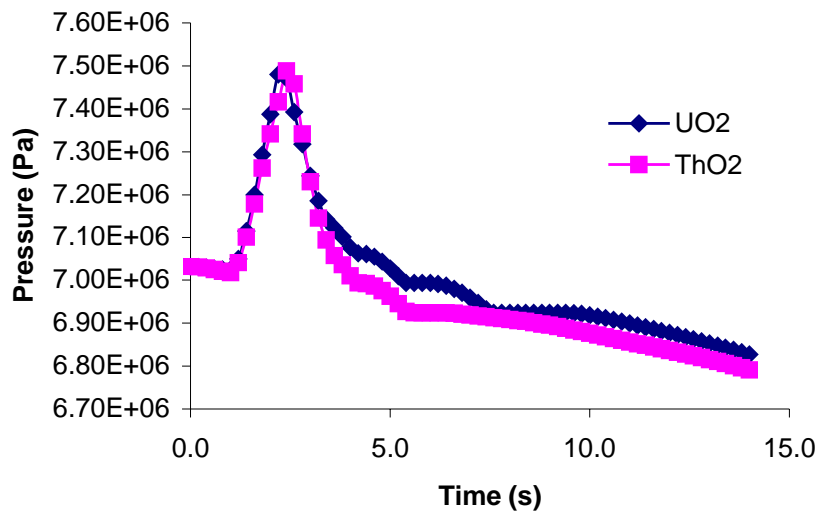


Figure 14. Pressure at the vessel dome during the main steam isolation valves closure transient

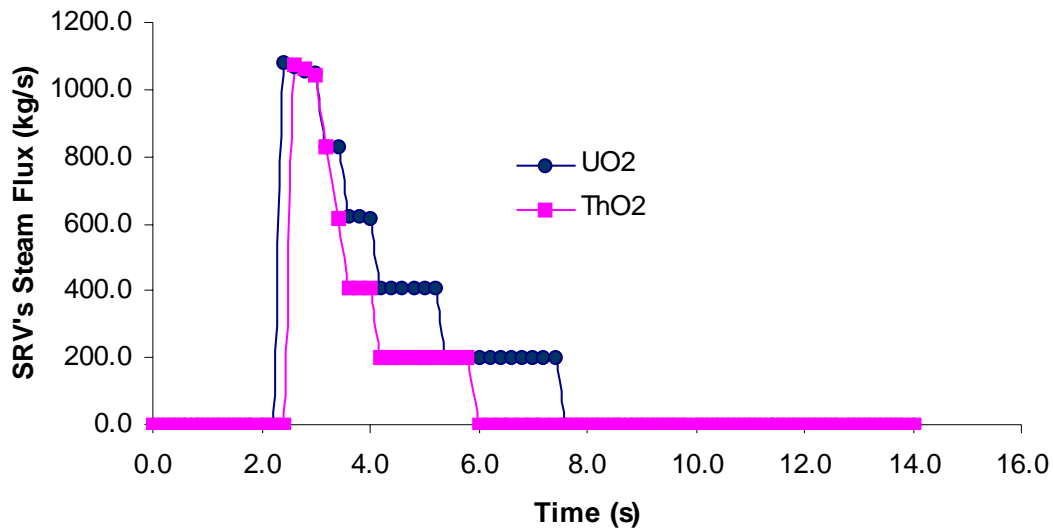


Figure 15. Steam Flux at the SRV's during the main steam isolation valves closure transient

TABLE III. Main parameters obtained from the stability analysis.

| Case* | Power (%) | Core flow (%) | Rod pattern | Boiling Length (m) |      | Frequency (Hz)  |      |
|-------|-----------|---------------|-------------|--------------------|------|-----------------|------|
|       |           |               |             | UO <sub>2</sub>    | Th   | UO <sub>2</sub> | Th   |
| 1     | 38.88     | 28.6          | 80          | 0.93               | 0.88 | 0.38            | 0.57 |
| 2     | 47.38     | 28.6          | 100         | 0.76               | 0.72 | 0.39            | 0.59 |
| 3     | 45.77     | 40.0          | 80          | 1.10               | 1.05 | 0.49            | 0.80 |
| 4     | 56.22     | 40.0          | 100         | 0.90               | 0.85 | 0.49            | 0.75 |
| 5     | 100       | 100           | 100         | 1.26               | 1.20 | 1.00            | > 1  |

\*Operational State

## CONCLUSIONS

A blanket-seed thorium-uranium fuel and a BWR equilibrium core were designed in this work. It can be concluded that such a core is feasible and comparable with an actual BWR uranium core. The analyzed parameters behave well but an optimization step is required to improve the blanket-seed assembly enrichment and the reload design. It must be emphasized the benefit of the thorium-uranium fuel assembly in terms of actinides reduction and plutonium in particular.

Other of the main conclusions of this work is that the dynamic behavior of the proposed thorium-uranium core is very close to the standard BWR, therefore no important changes are expected in the safety systems of the nuclear power station.

## ACKNOWLEDGEMENT

The authors acknowledge the support given by CONACyT through research projects 34657-U and 41592-Y and the National Autonomous University of Mexico through project PAPIIT-IN106803-2. One of the

authors (A. Núñez-Carrera) would like to thank the Nuclear Safety and Safeguards National Commission (Comisión Nacional de Seguridad Nuclear y Salvaguardias) for the support to perform this work.

## REFERENCES

1. X. Zhao, M. J. Driscoll, M. S. Kazimi, P. Hejzlar, "An Innovative ThO<sub>2</sub>-UO<sub>2</sub> Fuel for LWRs", *Trans. Am. Nucl. Soc.*, Milwaukee, USA, June 17-21, 2001, **84**, 235-236 (2001).
2. T. K. Kim, T. J. Downar, "Thorium Fuel in Tight Pitch LWR Lattices", *Trans. Am. Nucl. Soc.*, Milwaukee, USA, June 17-21, 2001, **84**, 236-238 (2001).
3. E. P. Lowen, K. D. Weaver, J. K. Hohorst, "Reactivity, Isotopics, and Thermal Steady-State Analysis of Homogeneous Thoria-Urania Fuels", *Nuclear Technology*, **137**, 97-110 (2002).
4. A. Galperin, P. Reichert, A. Radkowsky, "Thorium Fuel Cycle for Light Water Reactor - Reducing Proliferation Potential of Nuclear Power Fuel Cycle," *Science & Global Security*, Vol. 6, pp. 265-290 (1997).
5. M-H. Kim, Il-T. Woo, "Once-Through Thorium Fuel Cycle Options for the Advanced PWR Core", *Proceedings of the ANS Reactor Physics, Mathematics and Computation and Nuclear Criticality Safety, PHYSOR 2000 Topical Meeting*, Pittsburgh, USA, May 7-12, Proceedings on CD, (2000).
6. H. Etherington, *Nuclear Engineering Handbook*, Mc. Graw Hill Book Company, (1958).
7. J. Shackelford, W. Alexander, *The CRC Material Science and Engineering Handbook*, CRC Press, (1992).
8. Scandpower, User Manual for CM-PRESTO-91 (1992).
9. J. J. Casal, R. J. J. Stamm'ler, E. A. Villarino and A. A. Ferri, "HELIOS: Geometric capabilities of a new fuel assembly program", *Proc. Int. Topl. Mtg. Advances in Mathematics, Computations and Reactor Physics*, Pittsburgh, Pennsylvania. Vol. 2, p. 10.2.1 1-13, American Nuclear Society (1991).
10. Scandpower, User Manual for TABGEN (1992).
11. G. Espinosa, "Modelo de cinética y la termohidráulica del núcleo de un reactor tipo BWR para simulación de transitorio en tiempo real". *Mechanical Engineering M. Sc. Thesis*, CENIDET (1992).
12. R. Lahey and M. Podowski, "On the Analysis of various instabilities in two-phase flows". *Multiphase science and technology*, Vol. 5 (1990).
13. T. Nakajima., "Analysis of OECD MSLB Benchmark using coupled 3-D neutronics and thermal-hydraulics code SKETCH-INS/TRAC-P", *Technical Meeting on Progress in Development and Use of Coupled Codes for Accident Analysis*, November 26-28, Vienna, Austria, 2003.
14. G. Verdú et al., *FORSMARK 1 & 2 "Boiling Water Reactor Stability Benchmark, Time Series Analysis Method for Oscillations During BWR Operation."* *Final Report NEA/NSC/DOC(2001)2*, Nuclear Energy Agency OECD, June 2001.
15. "State of the Art Report on Boiling Water Reactor Stability (SOR on BWRs)", *NEA/CSNI/R (96)13*, Nuclear Energy Agency, OECD. Committee on the Safety of Nuclear Installations, January 1997.